

# Metal–Phosphorus Bonding in Fe(CO)<sub>4</sub>PR<sub>3</sub> Complexes. A Density Functional Study

Òscar González-Blanco and Vicenç Branchadell\*<sup>†</sup>

Departament de Química, Universitat Autònoma de Barcelona, Edifici Cn,  
08193 Bellaterra, Spain

Received June 23, 1997<sup>⊗</sup>

Fe(CO)<sub>4</sub>PR<sub>3</sub> complexes have been studied for R = H, Me, Ph, OMe, F, *i*-Pr, and NC<sub>4</sub>H<sub>4</sub> using density functional methods. The Fe–PR<sub>3</sub> bond has been analyzed in terms of steric and electronic effects. The results obtained show that the main contribution to the bond stems always from the  $\sigma$  donation, but phosphines can be classified into three groups depending on the relative magnitude of the  $\pi$ -back-donation contribution. Thus, PMe<sub>3</sub>, PPh<sub>3</sub>, and P(*i*-Pr)<sub>3</sub> can be considered as  $\sigma$ -donor ligands, PF<sub>3</sub> and P(NC<sub>4</sub>H<sub>4</sub>)<sub>3</sub> would be  $\sigma$ -donor/ $\pi$ -acceptor ligands, and PH<sub>3</sub> and P(OMe)<sub>3</sub> would correspond to intermediate cases.

## Introduction

Phosphorus(III) ligands play an important role in organometallic chemistry, since they are present in many transition-metal complexes.<sup>1–3</sup> By selection of the appropriate substituents on the PR<sub>3</sub> ligand, the steric and electronic properties of the complex can be modified within a broad range.

The interaction between a PR<sub>3</sub> ligand and a metal is usually described in terms of steric and electronic effects. The separation between both effects is not always straightforward, since they are interconnected. The steric size of a ligand is usually measured through the cone angle  $\theta$  introduced by Tolman.<sup>4</sup> Two excellent reviews have recently been devoted to methods for estimating steric requirements of ligands.<sup>5,6</sup> The electronic contribution to the M–P bond can be analyzed in terms of two factors: a  $\sigma$ -donation from the lone pair of the phosphorus ligand to the corresponding empty orbital of the metal fragment and a  $\pi$ -back-donation from the occupied orbitals of the metal to the virtual orbitals of appropriate symmetry in the PR<sub>3</sub> ligand. Several studies have been devoted to the nature of the donor and acceptor orbitals of the PR<sub>3</sub> ligands.<sup>7–9</sup> Xiao *et al.*<sup>7</sup> have analyzed the nature of the frontier orbitals of several PR<sub>3</sub> molecules, showing that the lowest energy acceptor orbital of these systems is mostly a 3p orbital on the P atom with an antibonding P–R character. This fact has been confirmed by the measurement of electron attachment energies of the unstable negative ions of PR<sub>3</sub> by electron transmission spectroscopy.<sup>8</sup>

Orpen *et al.*<sup>10–12</sup> have analyzed the geometries of several M–PR<sub>3</sub> complexes, providing evidence for the participation of P–R  $\sigma^*$  orbitals in the bonding.

Several parameters have been used to measure the donor/acceptor properties of PR<sub>3</sub> ligands. The  $\sigma$ -donor ability of PR<sub>3</sub> ligands has been related to their basicity. The gas-phase proton affinity, which would measure the Brønsted basicity, and the ionization energy, related to the Lewis basicity, usually follow similar trends.<sup>13</sup> The basicity of phosphines has also been related to the heats of protonation of M–PR<sub>3</sub> complexes.<sup>14</sup> Drago<sup>15,16</sup> has rationalized the  $\sigma$ -donor strengths of phosphines by means of electrostatic and covalent substituent constants,  $E_B$  and  $C_B$ .

Electron donor/acceptor properties of PR<sub>3</sub> ligands have also been studied from the variation of CO stretching frequencies<sup>4</sup> and from <sup>13</sup>C NMR data<sup>17</sup> in families of transition-metal carbonyl compounds. On the basis of values of CO stretching frequencies in Ni(CO)<sub>3</sub>PR<sub>3</sub> complexes, Tolman<sup>4</sup> introduced the electronic parameter  $\chi$  associated with each substituent of the PR<sub>3</sub> ligand. The values obtained for this parameter show that the donor/acceptor ratio increases for different R substituents in the order halogen < alkoxy < aryl < alkyl.

This donor/acceptor ratio should be the result of changes in the  $\sigma$ - and  $\pi$ -contributions to the bonding. Several authors have proposed methods to distinguish between  $\sigma$ -donor and  $\pi$ -acceptor contributions to the M–P bond.<sup>18–24</sup> Giering *et al.*<sup>21,22</sup> have used the cor-

<sup>†</sup> E-mail: vicenc@klngon.uab.es. FAX: +34 3 581 2920.

<sup>⊗</sup> Abstract published in *Advance ACS Abstracts*, November 1, 1997.

(1) Collman, J. P.; Hegedus, L. C.; Norton, J. R.; Finke, R. G. *Principles and Applications of Organotransition Metal Chemistry*; University Science Books: Mill Valley, CA, 1987.

(2) Crabtree, R. H. *The Organometallic Chemistry of the Transition Metals*; Wiley: New York, 1988.

(3) McAuliffe, C. A.; Mackie, A. G. In *Encyclopedia of Inorganic Chemistry*; King, R. B., Ed.; Wiley: New York, 1994; pp 2989–3010.

(4) Tolman, C. A. *J. Am. Chem. Soc.* **1970**, *92*, 2953.

(5) Brown, T. L.; Lee, K. J. *Coord. Chem. Rev.* **1993**, *128*, 89.

(6) White, D.; Coville, N. J. *Adv. Organomet. Chem.* **1994**, *36*, 95.

(7) Xiao, S.-X.; Troglor, W. C.; Ellis, D. E.; Berkovitch-Yellin, Z. *J. Am. Chem. Soc.* **1983**, *105*, 7033.

(8) Tossell, J. A.; Moore, J. H.; Giordan, J. C. *Inorg. Chem.* **1985**, *24*, 1100.

(9) Rolke, J.; Brion, C. E. *Chem. Phys.* **1996**, *207*, 173.

(10) Orpen, A. G.; Connelly, N. G. *J. Chem. Soc., Chem. Commun.* **1985**, 1310.

(11) Orpen, A. G.; Connelly, N. G. *Organometallics* **1990**, *9*, 1206.

(12) Dunne, B. J.; Morris, R. B.; Orpen, A. G. *J. Chem. Soc., Dalton Trans.* **1991**, 653.

(13) Dias, P. B.; Minas de Piedade, M. E.; Martinho Simões, J. A. *Coord. Chem. Rev.* **1994**, *135/136*, 737.

(14) Angelici, R. J. *Acc. Chem. Res.* **1995**, *28*, 51.

(15) Drago, R. S. *Organometallics* **1995**, *14*, 3408.

(16) Drago, R. S.; Joerg, S. J. *Am. Chem. Soc.* **1996**, *118*, 2654.

(17) Bodner, G. M.; May, M. P.; McKinney, L. E. *Inorg. Chem.* **1980**, *19*, 1951.

(18) Graham, W. A. G. *Inorg. Chem.* **1968**, *7*, 315.

(19) Treichel, P. M. *Inorg. Chem.* **1968**, *7*, 1942.

(20) Stelzer, O.; Unger, E. *Chem. Ber.* **1975**, *108*, 1246.

(21) Golovin, M. N.; Rahman, M. M.; Belmonte, J. E.; Giering, W. P. *Organometallics* **1985**, *4*, 1981.

(22) Rahman, M. M.; Liu, H.-Y.; Eriks, K.; Prock, A.; Giering, W. P. *Organometallics* **1989**, *8*, 1.

(23) Alyea, E. C.; Song, S. *Inorg. Chem.* **1992**, *31*, 4909.

(24) Wang, S. P.; Richmond, M. G.; Schwartz, M. *J. Am. Chem. Soc.* **1992**, *114*, 7595.

relation between electrochemical data, the  $pK_a$  of the conjugated acid of PR<sub>3</sub>, and CO stretching frequencies to classify PR<sub>3</sub> ligands into two different classes:  $\sigma$ -donors and  $\sigma$ -donor/ $\pi$ -acceptors. According to this classification, the  $\pi$ -acceptor ability increases in the order PMe<sub>3</sub> < PPh<sub>3</sub> < P(OMe)<sub>3</sub>. However,  $\pi$ -effects in PR<sub>3</sub> are small compared to those of strong  $\pi$ -acids such as CO. Ligand electrochemical parameters have also been used in conjunction with computed molecular electrostatic potentials to analyze the donor/acceptor capabilities of several ligands, including PPh<sub>3</sub> and P(OMe)<sub>3</sub>.<sup>25</sup> The results obtained show that both ligands have similar  $\pi$ -acceptor abilities. The  $\pi$ -acceptor ability of PR<sub>3</sub> ligands has also been studied from <sup>17</sup>O quadrupole coupling constants in W(CO)<sub>5</sub>PR<sub>3</sub> complexes,<sup>24</sup> showing that even PMe<sub>3</sub> has some  $\pi$ -acceptor character.

Giering *et al.*<sup>26–29</sup> have developed a method called quantitative analysis of ligand effects (QALE) that can be applied to the study of PR<sub>3</sub> coordination. In this method several physicochemical properties are related to the stereoelectronic properties of ligands through parameters such as  $\chi$  and  $\theta$ . Fernandez *et al.*<sup>30</sup> have shown that the electrostatic and covalent parameters introduced by Drago<sup>15,16</sup> are linear combinations of these QALE parameters.

The nature of the M–P bond can also be analyzed from the values of the M–P bond lengths.<sup>31–34</sup> Bresciani-Pahor *et al.*<sup>31,32</sup> have observed that the Co–P bond length in a series of PR<sub>3</sub> complexes increases with the bulkiness of the PR<sub>3</sub> ligand. On the other hand, determination of Fe–P bond lengths in sterically uncongested PR<sub>3</sub> complexes has shown that ligands with  $\pi$ -acid character, such as P(OR)<sub>3</sub>, present shorter values than pure  $\sigma$ -donor ligands.<sup>34</sup>

The metal–PR<sub>3</sub> bond has also been studied through theoretical calculations.<sup>35–46</sup> In a series of papers, Brown *et al.*<sup>38–42</sup> have developed a method for quantifying the steric requirements of PR<sub>3</sub> ligands based on molecular mechanics calculations. In this method a

parameter called ligand repulsive energy,  $E_R$ , is introduced. The values obtained for this parameter correlate well with the cone angles.

Pacchioni and Bagus<sup>43</sup> have reported a theoretical study of the metal–PR<sub>3</sub> (R = H, F, Me, OMe) interaction in several Pd complexes. According to their analysis of the bonding energy, the  $\sigma$ -basicity of PR<sub>3</sub> changes only slightly from one ligand to another. In contrast, there are significant variations in the  $\pi$ -acidity. Finally, Fantucci *et al.*<sup>45</sup> have analyzed the M–PR<sub>3</sub> bonding in Pt(PX<sub>3</sub>)<sub>2</sub> (X = H, F), finding that PF<sub>3</sub> should be classified as both a stronger  $\sigma$ -donor and  $\pi$ -acceptor than PH<sub>3</sub>.

Another aspect of M–PR<sub>3</sub> complexes relevant for theoretical calculations is the modelization of the PR<sub>3</sub> ligand. Häberlen and Rösch<sup>44</sup> have computed bond dissociation energies for several Au–PR<sub>3</sub> complexes, showing that the value obtained for PH<sub>3</sub> is notably different than the values corresponding to PMe<sub>3</sub> and PPh<sub>3</sub>. Similar results have recently been reported by Schmid *et al.*<sup>46</sup> for Rh–PR<sub>3</sub> complexes.

The purpose of this paper is to carry out a systematic study of the M–PR<sub>3</sub> bond for a series of PR<sub>3</sub> ligands in order to distinguish between steric and electronic effects and between  $\sigma$ - and  $\pi$ -interactions. We have chosen a  $C_{3v}$  Fe(CO)<sub>4</sub>PR<sub>3</sub> complex, since in this system the symmetry of the complex is the same as that of the isolated PR<sub>3</sub> ligand, and  $\sigma$ - and  $\pi$ -orbitals belong to different symmetry species. As PR<sub>3</sub> ligands we have considered PH<sub>3</sub>, PMe<sub>3</sub>, PPh<sub>3</sub>, P(OMe)<sub>3</sub>, P(*i*-Pr)<sub>3</sub>, and PF<sub>3</sub>, which offer a broad variation of both steric and electronic properties. We have also considered tris(pyrrol-1-yl)phosphine, P(NC<sub>4</sub>H<sub>4</sub>)<sub>3</sub>, which has been shown to present an important  $\pi$ -acceptor character.<sup>47</sup>

## Computational Details

All the calculations have been done using the ADF program.<sup>48–50</sup> The molecular geometries have been optimized using the method developed by Versluis and Ziegler.<sup>51</sup> Two different levels of calculation have been used in the geometry optimizations. In the most simple one, the local density approximation<sup>52</sup> (LDA) has been used, with the parametrization developed by Vosko *et al.*<sup>53</sup> In the highest level of calculation the gradient corrections to the exchange and correlation potentials developed by Becke<sup>54</sup> and Perdew,<sup>55</sup> respectively, have been used (BP). All the reported energies have been computed to include the gradient corrections. The 1s shell of C and O and the 1s2s2p shells of Fe and P have been treated by the frozen core approximation.<sup>49</sup> For the representation of the valence shells of C, O, and P we have used an uncontracted double- $\zeta$  basis set of Slater orbitals (STO) augmented with a set of 3d polarization functions. For H we have also used a double- $\zeta$  basis set augmented with a set of 2p polarization functions. In the geometry optimization of the systems containing PPh<sub>3</sub> the polarization functions of the C and H atoms have not been included. However, the energies have been recomputed to include these functions.

(25) Fielder, S. S.; Osborne, M. C.; Lever, A. B. P.; Pietro, W. J. *J. Am. Chem. Soc.* **1995**, *117*, 6990.

(26) Wilson, M. R.; Woska, D. C.; Prock, A.; Giering, W. P. *Organometallics* **1993**, *12*, 1742.

(27) Lorschach, B. A.; Bennett, D. M.; Prock, A.; Giering, W. P. *Organometallics* **1995**, *14*, 869.

(28) Lorschach, B. A.; Prock, A.; Giering, W. P. *Organometallics* **1995**, *14*, 1694.

(29) Bartholomew, J.; Fernandez, A. L.; Lorschach, B. A.; Wilson, M. R.; Prock, A.; Giering, W. P. *Organometallics* **1996**, *15*, 295.

(30) Fernandez, A.; Reyes, C.; Wilson, M. R.; Woska, D. C.; Prock, A.; Giering, W. P. *Organometallics* **1997**, *16*, 342.

(31) Bresciani-Pahor, N.; Calligaris, M.; Randaccio, L. *Inorg. Chim. Acta* **1980**, *39*, 173.

(32) Bresciani-Pahor, N.; Randaccio, L.; Toscano, P. J. *J. Chem. Soc., Dalton Trans.* **1982**, 1559.

(33) Wovkulich, M. J.; Atwood, J. L.; Canada, L.; Atwood, J. D. *Organometallics* **1985**, *4*, 867.

(34) Liu, H.-Y.; Eriks, K.; Prock, A.; Giering, W. P. *Organometallics* **1990**, *9*, 1758.

(35) Marynick, D. S. *J. Am. Chem. Soc.* **1984**, *106*, 4064.

(36) Blomberg, M. R. A.; Brandemark, U. B.; Siegbahn, P. E. M.; Mathisen, K. B.; Karlström, G. *J. Phys. Chem.* **1985**, *89*, 2171.

(37) Braga, M. *Inorg. Chem.* **1985**, *24*, 2702.

(38) Caffery, M. L.; Brown, T. L. *Inorg. Chem.* **1991**, *30*, 3907.

(39) Lee, K. J.; Brown, T. L. *Inorg. Chem.* **1992**, *31*, 289.

(40) Brown, T. L. *Inorg. Chem.* **1992**, *31*, 1286.

(41) Choi, M.-G.; Brown, T. L. *Inorg. Chem.* **1993**, *32*, 1548.

(42) Choi, M.-G.; Brown, T. L. *Inorg. Chem.* **1993**, *32*, 5603.

(43) Pacchioni, G.; Bagus, P. S. *Inorg. Chem.* **1992**, *31*, 4391.

(44) Häberlen, O. D.; Rösch, N. *J. Phys. Chem.* **1993**, *97*, 4970.

(45) Fantucci, P.; Polezzo, S.; Sironi, M.; Bencini, A. *J. Chem. Soc., Dalton Trans.* **1995**, 4121.

(46) Schmid, R.; Herrmann, W. A.; Frenking, G. *Organometallics* **1997**, *16*, 701.

(47) Moloy, K. G.; Petersen, J. L. *J. Am. Chem. Soc.* **1995**, *117*, 7696.

(48) ADF 2.2; Theoretical Chemistry, Vrije Universiteit, Amsterdam.

(49) Baerends, E. J.; Ellis, D. E.; Ros, P. *Chem. Phys.* **1973**, *2*, 41.

(50) te Velde, G.; Baerends, E. J. *J. Comput. Phys.* **1992**, *99*, 84.

(51) Versluis, L.; Ziegler, T. *J. Chem. Phys.* **1988**, *88*, 322.

(52) Gunnarsson, O.; Lundquist, I. *Phys. Rev.* **1974**, *B10*, 1319.

(53) Vosko, S. H.; Wilk, L.; Nusair, M. *Can. J. Phys.* **1980**, *58*, 1200.

(54) Becke, A. D. *Phys. Rev. A* **1988**, *38*, 3098.

(55) Perdew, J. P. *Phys. Rev. B* **1986**, *33*, 8822.

(56) Boys, S. F.; Bernardi, F. *Mol. Phys.* **1970**, *19*, 553.

(57) Rosa, A.; Ehlers, A. W.; Baerends, E. J.; Snijders, J. G.; te Velde, G. *J. Phys. Chem.* **1996**, *100*, 5690.

(58) Gilheany, D. G. *Chem. Rev.* **1994**, *94*, 1339.

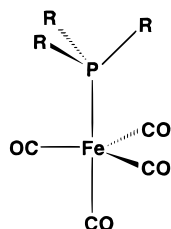


**Figure 1.** Schematic representation of the geometry of a  $\text{Fe}(\text{CO})_4\text{PR}_3$  complex.

**Table 1. Optimized Geometric Parameters<sup>a</sup> for the Free  $\text{PR}_3$  Molecules**

	P–R	R–P–R
H	1.432 (1.412)	91.9 (93.4)
Me	1.838 (1.847)	97.8 (98.6)
Ph	1.829 (1.828)	103.2 (103.0)
OMe	1.656	105.0
F	1.603 (1.570)	96.7 (97.8)
<i>i</i> -Pr	1.882	102.6
$\text{NC}_4\text{H}_4$	1.737	101.4

<sup>a</sup> Bond lengths are in angstroms, and bond angles are in degrees. Available experimental values for the isolated phosphines taken from ref 58 are given in parentheses.

Finally, for Fe we have used a triple- $\zeta$  basis set. The basis set superposition error (BSSE) on the computed bonding energies has been estimated through the counterpoise method.<sup>56,57</sup>

## Results and Discussion

Figure 1 schematically represents the geometry of a  $\text{Fe}(\text{CO})_4\text{PR}_3$  complex. The values of the most significant geometry parameters corresponding to the isolated  $\text{PR}_3$  ligands and to all the complexes are presented, respectively, in Tables 1 and 2. For  $\text{P}(\textit{i}\text{-Pr})_3$  we have considered the conformation in which all  $\text{CH}_3$  groups point toward the incoming metal fragment, as shown in **1**, in order to keep  $C_{3v}$  symmetry. For  $\text{P}(\text{OMe})_3$  we have considered the conformation in which all methyl groups are directed inward with respect to the 3-fold axis that passes through phosphorus, as shown is **2**. This conformation would be consistent with the value of the cone angle found in the literature ( $107^\circ$ ).<sup>60</sup>

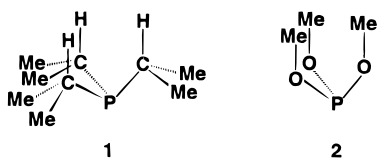


Table 1 shows that for the isolated  $\text{PR}_3$  molecules there is an excellent agreement between the computed and the experimental geometries. For the  $\text{Fe}(\text{CO})_4\text{PH}_3$  complex (see Table 2) we have optimized the geometry at two different levels of calculation. LDA underestimates the Fe–P bond length by more than  $0.07 \text{ \AA}$  with respect to BP, while for the Fe–C bonds the underestimation is  $0.05 \text{ \AA}$ . This difference in the optimized geometries has a small effect on the computed bond energies, as we will see below. For the  $\text{Fe}(\text{CO})_4\text{PPh}_3$  complex (Table 2), our results can be compared with the experimental crystal structure. The computed values of the Fe–P and Fe–C bond lengths are lower by about

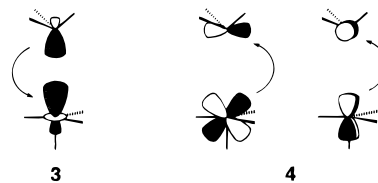
$0.05 \text{ \AA}$  than the experimental ones. If we assume that the LDA calculation underestimates these bond lengths by amounts similar to those in the  $\text{PH}_3$  complex, we may predict that a BP optimization of the  $\text{PPh}_3$  complex would lead to a Fe–P bond length slightly larger than the X-ray value.

We will analyze the bonding between  $\text{Fe}(\text{CO})_4$  and  $\text{PR}_3$  using the extended transition state method.<sup>61,62</sup> According to this method, the bond energy (BE) between two fragments can be decomposed into several contributions:

$$\text{BE} = -(\Delta E_{\text{prep}} + \Delta E_{\text{st}} + \Delta E_{\text{orb}})$$

$\Delta E_{\text{prep}}$  is the preparation energy term, i.e. the energy necessary to convert the fragments from their ground-state equilibrium geometries to the geometry and electronic state involved in the complex formation. This term can be split into contributions from both fragments. For  $\text{Fe}(\text{CO})_4$  we have considered the  $^3\text{B}_2$  ground state with the  $C_{2v}$  optimized geometry obtained by Li and Ziegler,<sup>63</sup> while in the complex, we have considered that this fragment is in a singlet state ( $^1\text{A}_1$  in  $C_{3v}$ ), so that its contribution to the preparation term will involve a triplet–singlet excitation and a geometry distortion.  $\Delta E_{\text{st}}$  is the steric interaction term. This term represents the interaction energy between the two “prepared” fragments with the electron densities that each fragment would have in the absence of the other fragment. This term can be split into an exchange repulsion or Pauli term ( $\Delta E_{\text{Pauli}}$ ) and an electrostatic term ( $\Delta E_{\text{elstat}}$ ). Finally, the orbital interaction term ( $\Delta E_{\text{orb}}$ ) represents the stabilization produced when the electron densities are allowed to relax.

The orbital interaction between  $\text{PR}_3$  and  $\text{Fe}(\text{CO})_4$  can be viewed as the consequence of two contributions: a  $\sigma$ -donation from the HOMO of  $\text{PR}_3$  to the LUMO of  $\text{Fe}(\text{CO})_4$  (**3**) and a  $\pi$ -back-donation involving the HOMO of  $\text{Fe}(\text{CO})_4$  and the LUMO of  $\text{PR}_3$  (**4**). The orbital



interaction term has been decomposed into several contributions:

$$\Delta E_{\text{orb}} = \Delta E_{\sigma} + \Delta E_{\pi} + \Delta E_{\text{syn}} + \Delta E_{\text{res}}$$

$\Delta E_{\sigma}$  is the  $\sigma$ -donation term and represents the stabilization produced when only the first  $\sigma$  virtual orbital of  $\text{Fe}(\text{CO})_4$  is included (**3**).  $\Delta E_{\pi}$  is the  $\pi$ -back-bonding term that represents the stabilization produced when only the first  $\pi$  virtual orbitals of  $\text{PR}_3$  are included (**4**).  $\Delta E_{\text{syn}}$ , the synergic term, is the additional stabilization produced when both interactions are allowed. Finally,  $\Delta E_{\text{res}}$  is the residual stabilization produced when the remaining virtual orbitals of both fragments are included. This term would take into account the polariza-

(59) Riley, P. E.; Davis, R. E. *Inorg. Chem.* **1980**, *19*, 159.

(60) Tolman, C. A. *Chem. Rev.* **1977**, *77*, 313.

(61) Ziegler, T.; Rauk, A. *Theor. Chim. Acta* **1977**, *46*, 1.

(62) Ziegler, T.; Rauk, A. *Inorg. Chem.* **1979**, *18*, 1558.

(63) Li, J.; Schreckenbach, G.; Ziegler, T. *J. Am. Chem. Soc.* **1995**, *117*, 486.

**Table 2. Optimized Geometry Parameters<sup>a</sup> of the Fe(CO)<sub>4</sub>PR<sub>3</sub> Complexes**

	H <sup>b</sup>	Me	Ph <sup>c</sup>	OMe	F	<i>i</i> -Pr	NC <sub>4</sub> H <sub>4</sub>
Fe–P	2.168 (2.252)	2.171	2.188 (2.244)	2.098	2.066	2.212	2.124
Fe–C <sub>ax</sub>	1.751 (1.799)	1.759	1.751 (1.795)	1.760	1.765	1.750	1.758
Fe–C <sub>eq</sub>	1.756 (1.811)	1.747	1.754 (1.794)	1.757	1.766	1.755	1.762
C <sub>ax</sub> –O <sub>ax</sub>	1.148 (1.156)	1.149	1.150 (1.139)	1.150	1.145	1.150	1.148
C <sub>eq</sub> –O <sub>eq</sub>	1.153 (1.160)	1.155	1.154 (1.143)	1.153	1.148	1.158	1.152
P–R	1.417 (1.418)	1.800	1.837 (1.831)	1.613	1.569	1.890	1.724
Fe–C <sub>eq</sub> –O <sub>eq</sub>	179.4 (179.7)	175.0	179.7 (178.3)	178.9	178.6	174.5	179.0
P–Fe–C <sub>eq</sub>	88.3 (88.8)	85.2	87.9 (88.8)	86.9	89.5	90.8	89.3
R–P–R	99.0 (98.5)	104.2	105.0 (103.9)	107.4	98.0	102.9	103.1

<sup>a</sup> Bond distances are in angstroms, and bond angles are in degrees. <sup>b</sup> Values in parentheses obtained at a BP level of calculation. <sup>c</sup> Experimental values given in parentheses are taken from ref 59.

**Table 3. Decomposition of the Interaction Energy<sup>a</sup> between PR<sub>3</sub> and a Model Fe(CO)<sub>4</sub> Fragment**

	H	Me	Ph	OMe	F	<i>i</i> -Pr	NC <sub>4</sub> H <sub>4</sub>
<i>E</i> <sub>Pauli</sub>	130.9	155.6	199.1	127.3	105.5	269.0	165.3
<i>E</i> <sub>elstat</sub>	–95.2	–126.6	–146.2	–98.8	–70.9	–175.9	–113.1
<i>E</i> <sub>st</sub>	35.7	29.0	52.9	28.5	34.6	93.1	52.2
<i>E</i> <sub>σ</sub>	–35.8	–40.8	–39.9	–33.6	–28.4	–44.3	–32.4
<i>E</i> <sub>π</sub>	–8.3	–7.0	–7.3	–9.2	–13.5	–7.7	–13.1
<i>E</i> <sub>syn</sub>	–9.2	–9.4	–8.9	–10.1	–12.9	–9.5	–12.8
<i>E</i> <sub>res</sub>	–26.4	–31.0	–43.8	–29.5	–26.3	–55.6	–34.1
<i>E</i> <sub>orb</sub>	–79.7	–88.2	–99.9	–82.4	–81.1	–117.1	–92.3
<i>E</i> <sub>st</sub> + <i>E</i> <sub>orb</sub>	–44.0	–59.2	–47.0	–53.9	–46.5	–24.0	–40.2

<sup>a</sup> See text for definitions; values in kcal mol<sup>–1</sup>.

**Table 4. Frontier Orbital Energies, Proton Affinities, Ionization Potentials, Tolman Electronic Parameters, and Cone Angles for the PR<sub>3</sub> Ligands**

R	<i>E</i> <sub>HOMO</sub> <sup>a</sup>	<i>E</i> <sub>LUMO</sub> <sup>a</sup>	PA <sup>b</sup>	<i>E</i> <sub>i</sub> <sup>c</sup>	χ <sup>d</sup>	cone angle <sup>e</sup>
H	–6.94	–0.25	789	9.87	8.3	87
Me	–5.58	0.32	950	8.06	2.85	118
Ph	–6.26	0.23 <sup>f</sup>	962	7.39	4.42	145
OMe	–6.66	–0.20	923	8.5	8.03	107
F	–8.40	–1.89			18.2	104
<i>i</i> -Pr	–5.47	0.02			1.15	160
NC <sub>4</sub> H <sub>4</sub>	–7.94	–1.77				

<sup>a</sup> Values in eV. <sup>b</sup> Values in kJ mol<sup>–1</sup> taken from ref 13. <sup>c</sup> Values in eV taken from ref 13. <sup>d</sup> Values in cm<sup>–1</sup> taken from ref 13. <sup>e</sup> Values in degrees taken from ref 60. <sup>f</sup> Energy of the LUMO + 2 orbital, since the LUMO is centered on the Ph ligands.

tion of both fragments that contributes to alleviate the steric repulsion between them.

We will first perform an analysis of the bonding using model geometries, in order to analyze the intrinsic electronic and steric properties of all phosphines and isolate them from effects due to changes in the geometries of the fragments. We will consider the interaction between a PR<sub>3</sub> molecule in its equilibrium geometry and in the same position occupied by PH<sub>3</sub> in the Fe(CO)<sub>4</sub>–PH<sub>3</sub> complex and a singlet Fe(CO)<sub>4</sub> fragment with the geometry corresponding to the Fe(CO)<sub>4</sub>PH<sub>3</sub> complex. In these cases the contribution of the Fe(CO)<sub>4</sub> fragment to the preparation energy term will have the same value in all complexes and has not been included. The results obtained are presented in Table 3. Table 4 presents the computed values for the HOMO and LUMO energies of the isolated PR<sub>3</sub> molecules as well as several parameters obtained from the literature, such as proton affinities, ionization potentials, Tolman electronic parameters, and cone angles.

Table 3 shows that the steric energy term increases in the order OMe < Me < F < H < NC<sub>4</sub>H<sub>4</sub> < Ph < *i*-Pr. There is a parallel variation in the absolute values of electrostatic and Pauli terms. The variation of the Pauli

term, i.e. the repulsive contribution to the steric energy term, follows the same trends as the values of the cone angles (Table 4), the only exception being PH<sub>3</sub>.

The absolute value of the σ-donation contribution to the orbital interaction term decreases in the order *i*-Pr > Me > Ph > H > OMe > NC<sub>4</sub>H<sub>4</sub> > F. With the only exception of PH<sub>3</sub>, this ordering is consistent with the values of *E*<sub>HOMO</sub>, proton affinities, and ionization potentials presented in Table 4. According to these results, proton affinity is a good measure of the σ-donor ability of PR<sub>3</sub> in a metal complex.

Regarding the π-back-donation contribution, Table 3 shows that the absolute value of this term decreases in the order F > NC<sub>4</sub>H<sub>4</sub> > OMe > H > *i*-Pr > Ph > Me. Again, with the only exception of PH<sub>3</sub>, this ordering is the same as the one corresponding to the values of *E*<sub>LUMO</sub> (Table 4).

The comparison between the σ- and π-contributions to the orbital interaction energy shows that all the PR<sub>3</sub> ligands studied are essentially σ-donor ligands. From the relative contributions of the σ- and π-terms we can distinguish between three different cases. The first one corresponds to “pure” σ-donor phosphines (PMe<sub>3</sub>, P(*i*-Pr)<sub>3</sub>, and PPh<sub>3</sub>), in which the contribution of the π-term is only about 17–18% of that of the σ-term. The second case would correspond to PF<sub>3</sub> and P(NC<sub>4</sub>H<sub>4</sub>)<sub>3</sub>, which can be considered as σ-donor/π-acceptor phosphines. In these cases the contribution of the π-term is greater than 40% of that corresponding to the σ-term. Finally, the third case would correspond to intermediate ligands (PH<sub>3</sub> and P(OMe)<sub>3</sub>), for which the contribution of the π-term is between 23 and 28% of the σ-contribution.

This ordering is in a good qualitative agreement with the donor/acceptor scales proposed by several authors.<sup>4,17,21,22</sup> In contrast, previous theoretical studies<sup>25,43,45</sup> obtained different results in some aspects. According to our results, the PR<sub>3</sub> ligands studied differ mainly in the σ-donor ability, while, with the exception of PF<sub>3</sub> and NC<sub>4</sub>H<sub>4</sub>, they are weak π-acceptors.<sup>43</sup> We conclude that PF<sub>3</sub> is weaker σ-donor than PH<sub>3</sub>,<sup>45</sup> Finally, P(OMe)<sub>3</sub> is a better π-acceptor than PPh<sub>3</sub>.<sup>25</sup>

The synergic contribution to the orbital interaction term is slightly larger for PF<sub>3</sub>, P(OMe)<sub>3</sub>, and P(NC<sub>4</sub>H<sub>4</sub>)<sub>3</sub> than for the other ligands, while the variation of the absolute value of the residual term follows the same trend as the steric term, except for PF<sub>3</sub>. The variation of the absolute value of Δ*E*<sub>st</sub> + Δ*E*<sub>orb</sub> follows the order Me > OMe > Ph > F > H > NC<sub>4</sub>H<sub>4</sub> >> *i*-Pr, as a consequence of both steric and orbital interactions.

Let us now consider the effects that take place when the geometries of the different complexes are optimized. The analysis of the bonding energy corresponding to the optimized geometries is presented in Table 5. If we

**Table 5.** Decomposition of the Bonding Energy<sup>a</sup> between PR<sub>3</sub> and Fe(CO)<sub>4</sub>

	H	Me	Ph	OMe	F	<i>i</i> -Pr	NC <sub>4</sub> H <sub>4</sub>
$E_{\text{prep}}(\text{PR}_3)$	1.8	4.7	1.4	5.5	4.8	2.4	2.5
$E_{\text{prep}}(\text{Fe}(\text{CO})_4)$	7.7	9.8	8.2	8.2	7.8	8.2	7.6
$E_{\text{Pauli}}$	138.9	189.9	188.8	177.2	147.0	172.2	179.8
$E_{\text{elstat}}$	-105.2	-153.7	-144.0	-136.3	-101.9	-138.0	-129.0
$E_{\text{st}}$	33.7	36.2	44.8	40.9	45.1	34.2	50.8
$E_{\sigma}$	-38.0	-49.7	-41.3	-40.8	-31.1	-40.1	-34.2
$E_{\pi}$	-7.4	-5.1	-5.5	-9.1	-15.8	-5.6	-12.9
$E_{\text{syn}}$	-8.8	-7.5	-7.6	-10.3	-15.1	-7.7	-13.0
$E_{\text{res}}$	-27.2	-40.1	-43.1	-38.8	-32.7	-38.2	-35.6
$E_{\text{orb}}$	-81.4	-102.4	-97.5	-99.0	-94.7	-91.6	-95.7
$E_{\text{st}} + E_{\text{orb}}$	-47.7	-66.2	-52.7	-58.1	-49.6	-57.4	-44.9
BE <sup>b</sup>	38.2 (35.3)	51.7 (45.3)	43.1 (34.8)	44.4 (37.0)	37.0 (28.8)	46.8 (38.0)	34.8 (26.4)

<sup>a</sup> See text for definitions; values in kcal mol<sup>-1</sup>. <sup>b</sup> Values in parentheses include the BSSE correction.

compare these results with the ones presented in Table 3, we can observe that the sum of the orbital and steric terms increases in absolute value upon geometry relaxation. In most cases, this increase is due to a diminution of the orbital term that overtakes the increase of the steric term. In contrast, for the bulkier phosphines, PPh<sub>3</sub> and P(*i*-Pr)<sub>3</sub>, the steric energy term decreases, while the orbital term becomes less stabilizing. For P(NC<sub>4</sub>H<sub>4</sub>)<sub>3</sub> we can also observe a diminution of the steric term, but the absolute value of the orbital term increases.

Regarding the components of the orbital energy term, we can observe that the  $\sigma$ -contribution increases in absolute value in all cases except for P(*i*-Pr)<sub>3</sub>. The  $\pi$ -acceptor term decreases in absolute value for most phosphines, while it remains almost unchanged for P(OMe)<sub>3</sub> and P(NC<sub>4</sub>H<sub>4</sub>)<sub>3</sub> and increases for PF<sub>3</sub>. As a result of these two effects, the  $\pi/\sigma$  ratio in the orbital interaction energy decreases in all cases except for PF<sub>3</sub> and P(*i*-Pr)<sub>3</sub>. However, the ordering of this ratio that has allowed us to distinguish between three different kinds of PR<sub>3</sub> ligands does not basically change due to the geometry relaxation.

Table 2 shows that the substitution of PH<sub>3</sub> by PMe<sub>3</sub>, PPh<sub>3</sub>, or P(*i*-Pr)<sub>3</sub> produces a lengthening in the Fe–P bond. In contrast, P(OMe)<sub>3</sub>, PF<sub>3</sub>, and P(NC<sub>4</sub>H<sub>4</sub>)<sub>3</sub> complexes have shorter Fe–P bonds. This result is consistent with the experimental observation that  $\pi$ -acceptor phosphines normally present shorter M–P bonds.<sup>34,47</sup> Upon complexation, the R–P–R bond angle of the phosphine increases, and so the R–P–Fe angle decreases. This distortion would produce an increase of the steric repulsion with the metal fragment. However, it leads to a destabilization of the HOMO of PR<sub>3</sub><sup>64</sup> and, hence, to an increase of the  $\sigma$ -donor ability of the PR<sub>3</sub> fragment. This increase in the value of the R–P–R angle is observed for all the complexes. However, the extent of this distortion strongly depends on the bulkiness of the R substituents. For PH<sub>3</sub>, the increase is 7.1°, while for P(*i*-Pr)<sub>3</sub> it is only 0.3°. The values of the P–R bond lengths also change upon complexation. In all cases except PPh<sub>3</sub> and P(*i*-Pr)<sub>3</sub> these bonds slightly shorten.

The replacement of PH<sub>3</sub> by PR<sub>3</sub> also produces a geometry distortion of the Fe(CO)<sub>4</sub> fragment. For Me, Ph, and OMe, the P–Fe–C<sub>eq</sub> angle decreases, so that

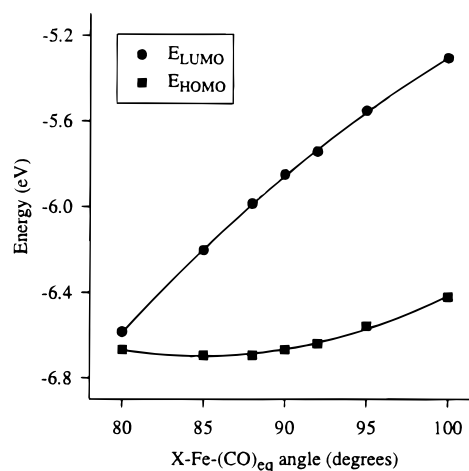


**Figure 2.** Variation of the frontier orbital energy of a  $C_{3v}$  Fe(CO)<sub>4</sub> fragment as the equatorial CO ligands bend over the vacant position. Bond lengths were taken from  $D_{3h}$  Fe(CO)<sub>5</sub> and kept frozen. The X–Fe–(CO)<sub>eq</sub> angle represents the angle of the vacant position (PR<sub>3</sub> in Figure 1), the Fe atom, and the equatorial carbonyls.

the equatorial CO ligands approach the PR<sub>3</sub> ligand. This distortion, which involves an increase in the steric repulsion, also leads to an enhancing of the  $\sigma$ -acceptor ability of the Fe(CO)<sub>4</sub> fragment. Figure 2 presents the variation of the total energy and the frontier orbital energies of a  $C_{3v}$  Fe(CO)<sub>4</sub> fragment versus the 3-fold-axis–Fe–C<sub>eq</sub> angle. We can observe that the diminution of this angle leads to an important lowering of the LUMO energy. The decrease of this angle is especially significant for PMe<sub>3</sub>, so that in this case, the  $\sigma$ -donation term is expected to be largely increased with respect to the model geometries, as we can confirm by comparing Tables 3 and 5. For the more  $\pi$ -accepting phosphine PF<sub>3</sub>, the 3-fold-axis–Fe–C<sub>eq</sub> angle slightly increases. This distortion would decrease the  $\sigma$ -acceptor ability of the metal fragment and slightly increase its  $\pi$ -donor character, since the HOMO of Fe(CO)<sub>4</sub> is slightly destabilized (see Figure 2). Therefore, for PF<sub>3</sub> we observe an increase of the contribution of the  $\pi$ -back-donation term. For P(*i*-Pr)<sub>3</sub>, the same kind of distortion is observed. However, it is the result of the large steric repulsion between both fragments. With regard to the values of the Fe–C bond lengths, Table 2 shows that the Fe–(CO)<sub>ax</sub> bond remains unchanged for Ph and *i*-Pr, while it is elongated in all other cases. The Fe–(CO)<sub>eq</sub>

(64) Albright, T. A.; Burdett, J. K.; Whangbo, M.-H. *Orbital Interactions in Chemistry*; Wiley: New York, 1985.

**Table 6. Net Charges<sup>a</sup> in the Different Fragments of the Fe(CO)<sub>4</sub>PR<sub>3</sub> Complexes**

	H	Me	Ph	OMe	F	<i>i</i> -Pr	NC <sub>4</sub> H <sub>4</sub>
Fe	0.267	0.459	0.245	0.394	0.297	0.471	0.235
PR <sub>3</sub>	0.428	0.417	0.456	0.278	0.186	0.440	0.318
CO <sub>ax</sub>	-0.131	-0.141	-0.119	-0.145	-0.091	-0.132	-0.084
CO <sub>eq</sub>	-0.188	-0.245	-0.194	-0.176	-0.131	-0.260	-0.156

<sup>a</sup> Values in au derived from a Mulliken population analysis.

bond length decreases for Me, remains almost unchanged for Ph, *i*-Pr, and OMe, and increases for F and NC<sub>4</sub>H<sub>4</sub>.

Table 6 presents the charge distribution obtained from a Mulliken population analysis in the Fe(CO)<sub>4</sub>PR<sub>3</sub> complexes in their optimized geometries. In all cases the charge on the Fe atom is positive. The maximum value is obtained for P(*i*-Pr)<sub>3</sub> and PMe<sub>3</sub>, followed by P(OMe)<sub>3</sub>. The charge on Fe does not reflect the donor/acceptor character of the PR<sub>3</sub> ligand. The charge on the axial CO ligand only slightly changes from one complex to another. In contrast, the charge on the equatorial CO ligands varies within a broader range. The variation of these charges follows the donor/acceptor properties of the PR<sub>3</sub> ligand. The  $\pi$ -back-donation to the CO ligands will be enhanced by strong  $\sigma$ -donor PR<sub>3</sub> ligands, while the  $\sigma$ -donation from CO to Fe will be enhanced by  $\pi$ -acceptors. PR<sub>3</sub> ligands that can be considered essentially as  $\sigma$ -donors (PMe<sub>3</sub> and P(*i*-Pr)<sub>3</sub>) will increase the electron density on the CO ligands. In contrast, PF<sub>3</sub> and P(NC<sub>4</sub>H<sub>4</sub>)<sub>3</sub>, which have an important  $\pi$ -acceptor character, will lead to lower electron densities on the CO ligands. This is the variation observed in the charges on the equatorial CO ligands.

Let us now consider the values of the M–PR<sub>3</sub> bond dissociation energies. The largest value, 45.3 kcal mol<sup>-1</sup>, is obtained for PMe<sub>3</sub>, while the smallest values, 28.8 and 26.4 kcal mol<sup>-1</sup>, correspond to PF<sub>3</sub> and P(NC<sub>4</sub>H<sub>4</sub>)<sub>3</sub>, respectively. The remaining PR<sub>3</sub> ligands present bond dissociation energies that vary within a range of 3.2 kcal mol<sup>-1</sup>. The comparison of these results and the values of the Fe–P bond length in the complex (Table 2) shows that there is no direct relationship between the strength of an M–PR<sub>3</sub> bond and the M–P bond length. This fact has already been observed in Ti–PR<sub>3</sub> complexes by Ernst *et al.*<sup>65</sup> For the PH<sub>3</sub> complex we have also computed the bond dissociation energy from the geometries optimized at the BP level. The result obtained is 37.0 kcal mol<sup>-1</sup>, 1.7 kcal mol<sup>-1</sup> larger than the value computed for the LDA geometry (see Table 5). The error introduced in the bond energy is less than 5% when LDA geometries are used.

There are no experimental data for the Fe–PR<sub>3</sub> bond dissociation energies in Fe(CO)<sub>4</sub>PR<sub>3</sub> complexes, but the variation of the computed values for this system can be compared with the variation of bond energies corresponding to other complexes containing the same PR<sub>3</sub> ligands.<sup>13</sup> In Mo(CO)<sub>3</sub>(PR<sub>3</sub>)<sub>3</sub> complexes, the Mo–PR<sub>3</sub> bond dissociation energies determined from solution calorimetric studies range from 30.2 kcal mol<sup>-1</sup> for PCl<sub>3</sub> to 38.9 kcal mol<sup>-1</sup> for P(OMe)<sub>3</sub><sup>66</sup> with the following variation: PCl<sub>3</sub> < PPh<sub>3</sub> < PMe<sub>3</sub>  $\approx$  P(OMe)<sub>3</sub>. The ordering in the PMe<sub>3</sub>/P(OMe)<sub>3</sub> pair changes in the Mo(CO)<sub>4</sub>(PR<sub>3</sub>)<sub>2</sub>

system, where the corresponding Mo–PR<sub>3</sub> bond energies are 43.2 and 40.5 kcal mol<sup>-1</sup>, respectively.<sup>67</sup> For Fe–PR<sub>3</sub> systems Nolan *et al.*<sup>68–70</sup> have measured enthalpies of reactions of (benzylideneacetone)Fe(CO)<sub>3</sub> with phosphines leading to Fe(CO)<sub>3</sub>(PR<sub>3</sub>)<sub>2</sub>, from which the variation of the Fe–P strength can be predicted. The results obtained indicate that the Fe–PMe<sub>3</sub> bond is stronger than the Fe–PPh<sub>3</sub> one by 6 kcal mol<sup>-1</sup>. In a similar study Li *et al.*<sup>71</sup> have shown that the Fe–P(*i*-Pr)<sub>3</sub> bond energy must be between those of Fe–PMe<sub>3</sub> and Fe–PPh<sub>3</sub>. The values that we have computed for the Fe(CO)<sub>4</sub>PR<sub>3</sub> complexes are in excellent agreement with these experimental observations.

Regarding the P(NC<sub>4</sub>H<sub>4</sub>)<sub>3</sub> ligand, reaction enthalpies measured by Li *et al.*<sup>72</sup> for substitution reactions involving Ru complexes suggest that the M–P(NC<sub>4</sub>H<sub>4</sub>)<sub>3</sub> bond is slightly stronger than the M–PPh<sub>3</sub> bond. Our results do not agree with this observation. However, it should be taken into account that the experimental reaction enthalpies correspond to processes in THF solution, while the computed values would correspond to the gas phase.

Finally, there is a question that arises in theoretical calculations of PR<sub>3</sub>-containing systems: modeling the PR<sub>3</sub> ligand. Schmid *et al.*<sup>46</sup> have recently shown that in Rh–PR<sub>3</sub> complexes the Rh–PMe<sub>3</sub> bond dissociation energy is 7.2 kcal mol<sup>-1</sup> higher than the corresponding PH<sub>3</sub> bond dissociation energy. In our case the difference is even larger (9.9 kcal mol<sup>-1</sup>). Therefore, PH<sub>3</sub> would be a bad model of PMe<sub>3</sub> in a theoretical calculation. The same authors suggest that PMe<sub>3</sub> could be used as a model for PPh<sub>3</sub>. However, our results indicate that the difference between Fe–PMe<sub>3</sub> and Fe–PPh<sub>3</sub> bond energies is 10.6 kcal mol<sup>-1</sup>, so that PMe<sub>3</sub> would not be a good model for PPh<sub>3</sub> either. The value of the M–PR<sub>3</sub> bond dissociation energy must be considered when model PR<sub>3</sub> ligands are used in the study of processes that involve the cleavage or formation of M–P bonds. In cases in which the PR<sub>3</sub> ligands act only as spectator ligands, steric and electron donor/acceptor properties should be considered.<sup>73–75</sup>

## Concluding Remarks

We have studied Fe(CO)<sub>4</sub>PR<sub>3</sub> complexes, considering different PR<sub>3</sub> ligands. The Fe–PR<sub>3</sub> bonding has been analyzed in terms of steric and electronic factors. In a first analysis, model geometries have been considered for the complexes, in order to separate the steric and electronic terms from effects that arise from changes in the geometries of the fragments upon complexation. This analysis shows that the main contribution to the Fe–P bond stems from the  $\sigma$ -donation but, depending on the  $\pi/\sigma$  ratio, we can classify phosphines into three groups: “pure”  $\sigma$ -donor phosphines (PMe<sub>3</sub>, P(*i*-Pr)<sub>3</sub>, and PPh<sub>3</sub>, with a ratio lower than 20%),  $\sigma$ -donor/ $\pi$ -acceptor

(65) Ernst, R. D.; Freeman, J. W.; Stahl, L.; Wilson, D. R.; Arif, A. M.; Nuber, B.; Ziegler, M. L. *J. Am. Chem. Soc.* **1995**, *117*, 5075.

(66) Nolan, S. P.; Lopez de la Vega, R.; Hoff, C. D. *Organometallics* **1986**, *5*, 2529.

(67) Mukerjee, S. L.; Nolan, S. P.; Hoff, C. D.; Lopez de la Vega, R. *Inorg. Chem.* **1988**, *27*, 81.

(68) Luo, L.; Nolan, S. P. *Organometallics* **1992**, *11*, 3483.

(69) Luo, L.; Nolan, S. P. *Inorg. Chem.* **1993**, *32*, 2410.

(70) Li, C.; Nolan, S. P. *Organometallics* **1995**, *14*, 1327.

(71) Li, C.; Stevens, E. D.; Nolan, S. P. *Organometallics* **1995**, *14*, 3791.

(72) Li, C.; Serron, S.; Nolan, S. P. *Organometallics* **1996**, *15*, 4020.

(73) Lin, Z.; Hall, M. B. *J. Am. Chem. Soc.* **1992**, *114*, 2928.

(74) Svensson, M.; Humbel, S.; Froese, R. D. J.; Matsubara, T.; Sieber, S.; Morokuma, K. *J. Phys. Chem.* **1996**, *100*, 19357.

(75) Jacobsen, H.; Berke, H. *Chem. Eur. J.* **1997**, *3*, 881.

phosphines (PF<sub>3</sub> and P(NC<sub>4</sub>H<sub>9</sub>)<sub>3</sub>, with a ratio of about 40–50%), and intermediate phosphines (PH<sub>3</sub> and P(OMe)<sub>3</sub>, with intermediate ratios).

When the geometries of the complexes are allowed to relax, two kinds of distortions are observed. For complexes with bulky PR<sub>3</sub> ligands, the geometry distortion leads to a diminution of the steric contribution to the interaction energy. On the other hand, for PMe<sub>3</sub>, P(OMe)<sub>3</sub>, and PF<sub>3</sub> the geometry distortion involves an increase in the steric repulsion that is overtaken by a more favorable orbital interaction. The  $\sigma$ -donation contribution increases in all cases except for P(*i*-Pr)<sub>3</sub>, while the  $\pi$ -back-donation contribution only increases for PF<sub>3</sub>. Regarding the bond dissociation energies, we

have found that the strongest Fe–P bond belongs to Fe(CO)<sub>4</sub>PMe<sub>3</sub> (45.3 kcal mol<sup>-1</sup>), while the weakest ones are found for Fe(CO)<sub>4</sub>P(NC<sub>4</sub>H<sub>9</sub>)<sub>3</sub> (26.4 kcal mol<sup>-1</sup>) and Fe(CO)<sub>4</sub>PF<sub>3</sub> (28.8 kcal mol<sup>-1</sup>). The remaining complexes lie in between and vary from one to another within a range of only 3.2 kcal mol<sup>-1</sup>.

**Acknowledgment.** This work has been financially supported by the DGICYT (Grant Nos. PB92-0621 and PB95-0640) and CIRIT (Grant No. SGR95-00401). O.G.-B. gratefully acknowledges the Spanish Ministry of Education and Science for a doctoral fellowship.

OM9705214